

Critical Angle for Electrically Driven Coalescence of Two Conical Droplets

James C. Bird,^{1,*} William D. Ristenpart,² Andrew Belmonte,³ and Howard A. Stone^{1,†}

¹*School of Engineering and Applied Sciences, Harvard University, Cambridge, Massachusetts 02138, USA*

²*Department of Chemical Engineering and Materials Science and Department of Food Science and Technology, University of California at Davis, Davis, California 95616, USA*

³*W.G. Pritchard Laboratories, Department of Mathematics, Pennsylvania State University, University Park, Pennsylvania 16802, USA*
(Received 6 January 2009; revised manuscript received 10 July 2009; published 16 October 2009)

Oppositely charged drops attract one another and, when the drops are sufficiently close, electrical stresses deform the leading edges of each drop into cones. We investigate whether or not the liquid cones coalesce immediately following contact. Using high-speed imaging, we find that the coalescence behavior depends on the cone angle, which we control by varying the drop size and the applied voltage across the drops. The two drops coalesce when the slopes of the cones are small, but recoil when the slopes exceed a critical value. We propose a surface energy model (volume-constrained area minimization) to describe the transition between these two responses. The model predicts a critical cone angle of 30.8° , which is in good agreement with our measurements.

DOI: 10.1103/PhysRevLett.103.164502

PACS numbers: 47.55.df, 47.55.nk, 47.65.-d

When two drops of the same liquid come into contact, we expect them to coalesce because the combined drop minimizes the surface energy [1]. Accordingly, when drops fail to coalesce, the focus is typically on phenomena that prevent direct contact. For example, surfactant [2] and colloidal [3] coatings prevent the drops from contacting, while dynamic processes such as evaporation [4] or vibration [5] maintain a layer of immiscible fluid between the drops. If this fluid layer is penetrated by a meniscus bridge connecting the drops, coalescence is typically assumed to proceed. However, oppositely charged drops placed in sufficiently large electric fields fail to coalesce *even* when the two drops directly contact [6,7]. To interpret this noncoalescence, we develop a theoretical model based on the shape of the meniscus bridge and the local capillary pressure within this region. In addition, we provide an extensive set of experimental data that are in good agreement with the theoretical predictions.

Electric fields cause liquid droplets to develop conical structures oriented in the direction of the field [8–12]. Commonly referred to as Taylor cones [8,13,14], these structures result from a balance of charge induced pressure from the applied electric field and capillary pressure resisting interfacial deformation. The balance of these two effects is quantified by the nondimensional electrocapillary number, $\mathcal{E}_c = \frac{\epsilon\epsilon_0 E^2 a}{\gamma}$, where $\epsilon\epsilon_0$ is the permittivity of the liquid, E is the magnitude of the electric field, a is the radius of the drop, and γ is the surface tension. At sufficiently high values of \mathcal{E}_c , an uncharged single drop will develop two opposing conical tips aligned with the field. Similarly, drop pairs also deform in an electric field. The dynamics of a pair of drops aligned with an electric field have been investigated for both inviscid [15–18] and viscous responses [19–21]. Each drop enhances the deformation of the other, and below a critical separation distance, the drops become unstable and rapidly converge.

Numerical simulations suggest that inviscid drops develop rounded, but highly distorted, tips as they converge, and that these tips become pointed at contact [18]. Unlike Taylor cones, which have a well-defined angle, the conical tips in the inviscid simulations show cone angles that *vary* with the electrocapillary number.

None of the above studies considered the behavior of drop pairs after contact. Thus, we begin by showing experimentally (Fig. 1) that above a critical field strength, water droplets deform into sufficiently steep cones and fail to coalesce. We argue that the dominant role of the electric field is to distort the drops prior to contact, and that the subsequent dynamics depend predominantly on capillarity. The coalescence-noncoalescence transition we describe acts as a “gate,” preventing drops of a particular size and interfacial charge from coalescing. The goal of this Letter is to characterize this transition, as well as provide additional insight into the underlying physics.

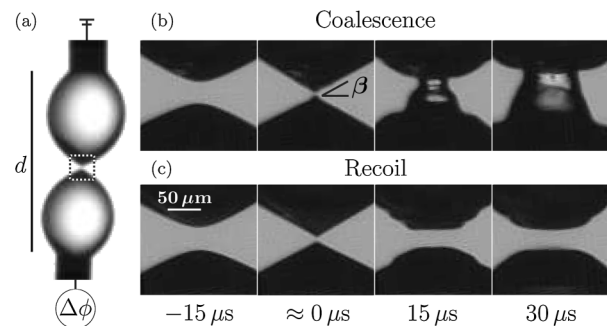


FIG. 1. (a) A voltage $\Delta\phi$ is applied across a pair of drops that are suspended on needles separated by a distance d (here $d = 1.9$ mm). (b) Prior to contact, each drop deforms into a cone with angle β . At lower voltages, the drops immediately coalesce; $\Delta\phi = 815$ V. (c) At higher voltages, the drops contact and then recoil; $\Delta\phi = 822$ V. Note the slight misalignment of the needles in (a) demonstrates the robustness of this phenomenon.

Our experimental setup consists of two stainless steel needles separated by a gap d [Fig. 1(a)]. A power generator supplies a controllable voltage $\Delta\phi$ across the needles. After the voltage is applied, deionized water (conductivity $\sigma = 4 \mu\text{S}/\text{cm}$) is slowly injected through the needles to form nearly spherical drops; the speed due to injection is $\approx 100 \mu\text{m}/\text{s}$. Once the drops reach a critical size, the drops become unstable and electric forces bring them together (speed $\approx 1 \text{ m}/\text{s}$). The onset of the instability and the subsequent dynamics are recorded at 67 000 frames per second with a Phantom V7 camera and analyzed with custom-written MATLAB algorithms. These steps are repeated for different gap sizes and voltages. To test the effects of the dielectric strength of the surrounding gas, we conducted experiments in three gases: air, helium, and sulfur hexafluoride.

The high-speed images demonstrate that the drops generally deform into a double cone near the point of contact (Fig. 1). We observe one of two distinct behaviors after the drops contact. At sufficiently low voltages, the drops approach, contact in the shape of a double cone, and generate a growing fluid neck that leads to coalescence [Fig. 1(b)]. In contrast, at sufficiently high voltages, the drops deform, contact in the shape of a double cone, and then quickly repel [Fig. 1(c)]. After the drops initially recoil, they approach a second time, presumably due to charge accumulation from the voltage source. Often the drops will no longer be conical during the second contact and will coalesce (see supplemental movie [22]). The implication is that noncoalescence is due to the shape of the interface rather than the strength of the field. The recoil and subsequent coalescence typically occur within a millisecond and therefore might explain why this phenomenon has not been reported previously. Here, we focus on the initial dynamics following the first contact.

The cone angle β is positively correlated with the applied voltage and negatively correlated with the needle separation (Fig. 2). When no voltage is applied ($\Delta\phi = 0$), the drops are nearly spherical and $\beta = 0$. For a given separation distance, there is a critical voltage when the drops no longer coalesce. At the highest voltages in our study, we observe a visible gap between the two surfaces prior to recoil. Because of limitations in frame rate, we cannot discern drops that contact between frames from those that do not contact. In our analysis, we determine β by estimating the angle assuming contact in these situations.

The coalescence between two oppositely charged droplets is expected, whereas the recoil is not. We suggest three mechanisms that could lead to this type of transition. First, high voltage may cause dielectric breakdown in the gas. If sufficient charge passed through the surrounding gas, the conical drops could neutralize prior to contact and recoil under the influence of surface tension. We tested the breakdown hypothesis directly in our setup by surrounding the liquid drops with gases that have noticeably different dielectric strengths. For each gas, we measured the minimum voltage required for a spark to be visually observed across

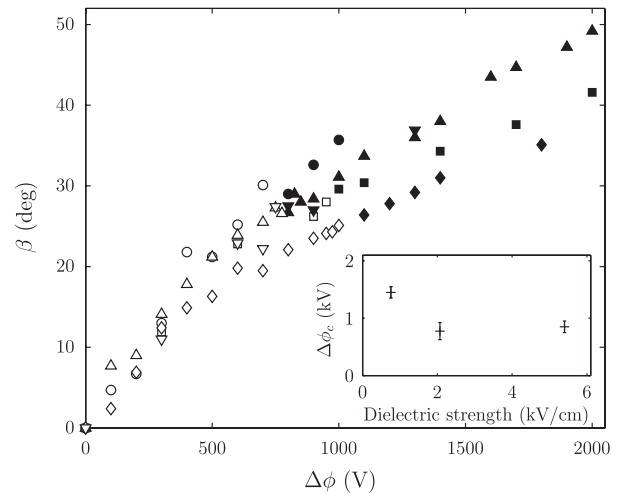


FIG. 2. The cone angle β varies based on the voltage and size of the drops. After contact, the drops either coalesce (open symbols) or recoil (closed symbols). The coalescence-recoil transition for deionized water drops at various needle separations, $d = 1.9 \text{ mm}$ (\circ, \bullet), 4.3 mm (\square, \blacksquare), and 5.1 mm (\diamond, \blacklozenge), occurs at different voltages, yet at similar cone angles. These features are consistent with previously reported data that focus on varying conductivity, $\sigma = 4 \mu\text{S}/\text{cm}$, $d = 2.4 \text{ mm}$ ($\triangle, \blacktriangle$), and $\sigma = 163 \mu\text{S}/\text{cm}$, $d = 2.8 \text{ mm}$ ($\nabla, \blacktriangledown$) [6]. Inset: The critical voltage between coalescence and recoil decreases, rather than increases, with the dielectric strength of surrounding gas.

the bare needles. Dielectric strengths of 0.76, 2.1, and $5.4 \text{ kV}/\text{mm}$ were recorded for helium, air, and sulfur hexafluoride, respectively, which is consistent with reported values [23]. If dielectric breakdown of the gas were responsible for the coalescence-recoil transition, then an increase in the dielectric strength of the gas would require a larger critical voltage $\Delta\phi_c$ to bring about the transition. However, our results (Fig. 2 inset) contradict this hypothesis.

The second possibility is that the recoil is a consequence of Joule heating. Once the drops contact, the charge equilibration could significantly heat the liquid in the neck region, leading to Marangoni effects or complete vaporization. Because Joule heating is proportional to conductivity, the critical voltage would also depend on the fluid conductivity for the recoil mechanism to be Joule heating related. However, there is no significant difference in the critical voltage when the fluid conductivity is varied between 4 and $163 \mu\text{S}/\text{cm}$ (Fig. 2) [6].

We propose a third possibility in which the coalescence-recoil transition is a consequence of the drop geometry. In existing models of coalescence and breakup, the dynamics are often explained by the shape of the neck region [24]. When two spherical drops touch, the contact generates capillary waves, which create an expanding liquid neck between the drops [25]. The negative curvature across the neck is much larger than the positive curvature around the neck, leading to lower fluid pressure in the neck than in the center of the drop. This capillary pressure difference drives

fluid into the meniscus resulting in drop coalescence [Fig. 3(a)]. In contrast, the instability in a liquid thread leads to a neck region with a negative curvature across the neck that is much smaller than the positive curvature around the neck [Fig. 3(b)]: the capillary pressure in the neck is positive, creating a flow away from the region and eventually causing the thread to break up. These physical arguments suggest that a coalescence-breakup transition may occur for conical drops, as the geometry typically has comparable curvatures across and around the neck [Fig. 3(c)]. We now estimate at what angle this transition would occur.

A two-dimensional analog of the coalescing cones has been solved numerically and leads to a self-similar neck with height w that grows as $w \sim (\frac{\gamma t^2}{\rho})^{1/3}$, where t is time and ρ is the fluid density [26]. By extension, we expect that in three-dimensions, the interplay of inertia and capillarity also leads to a self-similar, axisymmetric neck region, the precise shape of which requires detailed numerical analysis beyond the scope of this Letter. Unlike the planar analog, the axisymmetric profile has radial curvature that can prevent coalescence. Here, we approximate this self-similar profile as the geometry that minimizes surface energy while conserving volume, as this provides a unique shape that exists for any cone-angle and appears qualitatively similar to the shapes observed from experiments. Moreover, we expect that a minimal surface profile would become more accurate near the transition point as inertial forces change direction.

Figure 3(c) is a schematic of our quasistatic model for coalescence, in which we have normalized the neck region by w . For a given cone angle, β , the fluid is redistributed within the neck volume V so as to minimize the neck surface area S . We minimize the energy functional $F = \gamma S - pV$, where p is an unknown constraint constant that physically corresponds to the capillary pressure. Using the Euler-Lagrange relation, we find that the dimensionless axisymmetric profile $\tilde{r}(z/w)$ must satisfy

$$1 + \tilde{r}'^2 = \left(\frac{\tilde{r}}{k + \frac{pw}{2\gamma} \tilde{r}^2} \right)^2. \quad (1)$$

The solution to this differential equation has three unknown constants (k , p and one integration constant); this

necessitates three boundary conditions. We impose that the neck connects with the unperturbed fluid, $\tilde{r}(\pm 1) = \cot\beta$, and we require that the volume of the neck, $\int_{-1}^1 \pi \tilde{r}^2 d(\frac{z}{w})$, is equal to the initial volume of the perturbed region, $\frac{2\pi}{3} \cot^2\beta$ [Fig. 3(c)].

There is a critical angle β_c where the capillary pressure, p , switches signs. By solving (1) with $p = 0$ and satisfying the boundary conditions, we find that

$$\beta_c = \cot^{-1}[k \cosh(1/k)], \quad (2)$$

where $6 = 4\cosh^2(1/k) - 3k \sinh(2/k)$.

The numerical solution to (2) is $k \approx 0.582$, leading to a critical angle $\beta_c \approx 30.8^\circ$ and slope of the cone, $\tan\beta_c \approx 0.596$. We note that in a study of electrically mediated bouncing of oppositely charged drops [6], a crude capillary pressure model yielded a critical angle 45° . The detailed analysis of the full curvature presented here predicts an angle ($\approx 31^\circ$) that is in good agreement with the experimental transition in Fig. 2.

In this coalescence model, the electric field simply sets the cone angle; after contact, the proposed dynamics is independent of ion flow. This attribute of the model is consistent with two observations. First, the observed transition is independent of the fluid conductivity, whereas ion flow is generally not. Second, as shown in Fig. 4, the data in Fig. 2 collapse on to a master curve when rescaled by the electrocapillary number $\mathcal{E}_c = \frac{\epsilon\epsilon_0(\Delta\phi)^2 a}{\gamma d^2}$. Note that the electric field E in the earlier definition of \mathcal{E}_c has been replaced by $\frac{\Delta\phi}{d}$. Here, we show that the transition occurs for $\mathcal{E}_c \sim O(1)$ (Fig. 4) indicating the importance of the cone angle, as the shape of the interface depends on the balance of electric and capillary forces. The role of the electric field implies that whenever conical drops contact, the cone angle will determine whether or not the drops coalesce regardless of whether the cone angle was established by electrical hydrodynamics or by some other field, such as flow [27].

As a final remark, we discuss the shape of the conical drop near contact. Figure 4 demonstrates that the cone slope is $\tan\beta \approx 0.7\mathcal{E}_c^{1/2}$. Although we are currently unable to offer an analytic explanation, the results are nearly

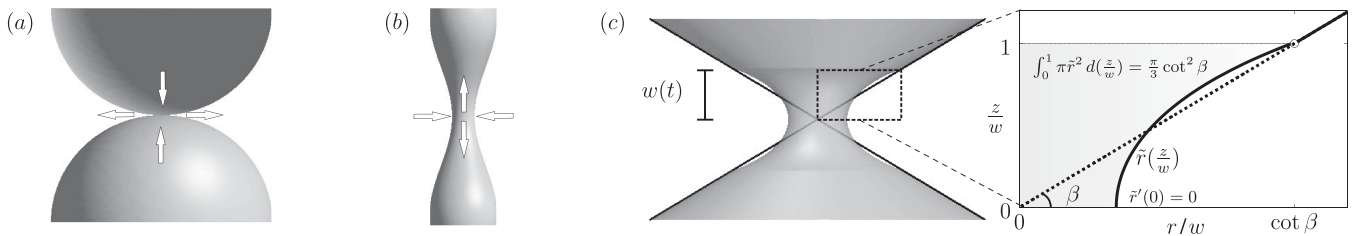


FIG. 3. (a) When two spherical drops contact, the curvature of the neck leads to a low local liquid pressure resulting in inward flow and coalescence. (b) The local curvature in an unstable liquid thread leads to a high pressure resulting in outward flow and pinch off. (c) We propose that immediately after two conical drops contact, there is a self-similar neck region, which we approximate as a volume-conserving minimal surface. We then calculate if the resulting curvature raises or lowers the local pressure, which is responsible for the resulting fluid motion.

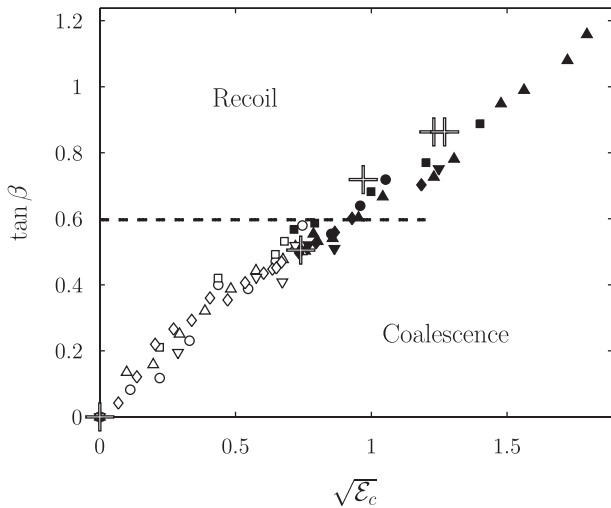


FIG. 4. The data presented in Fig. 2 collapse on to a master curve when plotted in terms of the electrocapillary number, \mathcal{E}_c . The results from our model (dotted line) predict the transition between coalescence and recoil reasonably well. The angles we observe are also consistent with past numerical simulations (five data points as +) [18].

identical to the angles that we have extracted from illustrations of the simulations reported by Brazier-Smith *et al.* [18], provided that we take the simulated electric field $E = \frac{\Delta\phi}{d}$. There are two implications from this finding. First, the results from our experiments can be extended to the setup of the simulations, which consisted of a constant electric field across two inviscid drops freely suspended in a fluid of constant pressure. Second, the similarity between the experiments and simulations provide additional evidence that the drops make contact. In [18], the deformed drops contacted when $\sqrt{\mathcal{E}_c} \leq 1.2$, which corresponded to $\beta \leq 40.1^\circ$, or $\tan\beta \leq 0.84$. Therefore, we expect that the pair of drops in our experiments also make contact when $\beta \leq 40.1^\circ$, even when these drops subsequently recoil. At higher values of \mathcal{E}_c , the simulated drops became unstable prior to contact, consistent with electrospaying [8,18]. Thus, we conclude that electrospaying may play a role in the recoil when $\sqrt{\mathcal{E}_c} > 1.2$.

We have found that above a critical electrocapillary number, a pair of drops aligned with an electric field no longer coalesce. By varying the drop size and the dielectric breakdown of the surrounding gas, we are able to evaluate potential mechanisms to describe this phenomenon. The results suggest that the transition between coalescence and recoil is due to the local curvature of the neck region, and our analytical model predicts this transition well. The findings are helpful in determining the conditions when charged drops, or drop pairs in electric fields, will coalesce. Because the transition appears to depend predominantly on geometry, a similar phenomenon may occur whenever fluid cones contact.

We thank L. Courbin for helpful discussions. We also thank the NSF via the Harvard MRSEC (DMR-0820484)

and IGERT programs for support of this research.

*jbird@fas.harvard.edu

†Present address: Department of Mechanical and Aerospace Engineering, Princeton University, Princeton, NJ 08544, USA;

hastone@princeton.edu

- [1] P. G. de Gennes, F. Brochard-Wyart, and D. Quéré, *Capillarity and Wetting Phenomena* (Springer, New York, 2004).
- [2] Y. Amarouchene, G. Cristobal, and H. Kellay, *Phys. Rev. Lett.* **87**, 206104 (2001).
- [3] R. Aveyard, B. P. Binks, and J. H. Clint, *Adv. Colloid Interface Sci.* **100–102**, 503 (2003).
- [4] M. A. Weilert, D. L. Whitaker, H. J. Maris, and G. M. Seidel, *Phys. Rev. Lett.* **77**, 4840 (1996).
- [5] Y. Couder, S. Protiere, E. Fort, and A. Boudaoud, *Nature (London)* **437**, 208 (2005).
- [6] W. D. Ristenpart, J. C. Bird, A. Belmonte, F. Dollar, and H. A. Stone, *Nature (London)* **461**, 377 (2009).
- [7] A. R. Thiam, N. Bremond, and J. Bibette, *Phys. Rev. Lett.* **102**, 188304 (2009).
- [8] G. Taylor, *Proc. R. Soc. A* **280**, 383 (1964).
- [9] D. A. Saville, *Annu. Rev. Fluid Mech.* **29**, 27 (1997).
- [10] H. A. Stone, J. R. Lister, and M. P. Brenner, *Proc. R. Soc. A* **455**, 329 (1999).
- [11] L. Oddershede and S. R. Nagel, *Phys. Rev. Lett.* **85**, 1234 (2000).
- [12] R. T. Collins, J. J. Jones, M. T. Harris, and O. A. Basaran, *Nature Phys.* **4**, 149 (2008).
- [13] J. R. Melcher and G. I. Taylor, *Annu. Rev. Fluid Mech.* **1**, 111 (1969).
- [14] J. F. de la Mora, *Annu. Rev. Fluid Mech.* **39**, 217 (2007).
- [15] J. Latham and I. W. Roxburgh, *Proc. R. Soc. A* **295**, 84 (1966).
- [16] G. Taylor, *Proc. R. Soc. A* **306**, 423 (1968).
- [17] P. R. Brazier-Smith, *Phys. Fluids* **14**, 1 (1971).
- [18] P. R. Brazier-Smith, S. G. Jennings, and J. Latham, *Proc. R. Soc. A* **325**, 363 (1971).
- [19] X. G. Zhang, O. A. Basaran, and R. M. Wham, *AIChE J.* **41**, 1629 (1995).
- [20] J. C. Baygents, N. J. Rivette, and H. A. Stone, *J. Fluid Mech.* **368**, 359 (1998).
- [21] A. Fernandez, G. Tryggvason, J. Che, and S. L. Ceccio, *Phys. Fluids* **17**, 093302(2005).
- [22] See EPAPS Document No. E-PRLTAO-103-024944 for a supplemental movie. For more information on EPAPS, see <http://www.aip.org/pubservs/epaps.html>.
- [23] *CRC Handbook of Chemistry and Physics, Internet Version 2007*, edited by D. R. Lide (Taylor and Francis, Boca Raton, FL, 2007), 87th ed.
- [24] J. Eggers, J. R. Lister, and H. A. Stone, *J. Fluid Mech.* **401**, 293 (1999).
- [25] M. M. Wu, T. Cubaud, and C. M. Ho, *Phys. Fluids* **16**, L51 (2004).
- [26] J. B. Keller, P. A. Milewski, and J. M. Vanden-Broeck, *Eur. J. Mech. B, Fluids* **19**, 491 (2000).
- [27] N. Bremond, A. R. Thiam, and J. Bibette, *Phys. Rev. Lett.* **100**, 024501 (2008).